Available online at www.sciencedirect.com
ScienceDirect
Journal of Power Sources 161 (2006) 47–53
JOURNAL OF POWER SOURCES
www.elsevier.com/locate/jpowsour

Multi-walled carbon nanotubes based Pt electrodes prepared with in situ ion exchange method for oxygen reduction

Yuyan Shao, Geping Yin*, Jiajun Wang, Yunzhi Gao, Pengfei Shi

Department of Applied Chemistry, Harbin Institute of Technology, PO Box 411, Harbin 150001, China

Received 15 February 2006; received in revised form 14 March 2006; accepted 28 March 2006
Available online 5 May 2006

Abstract

Multi-walled carbon nanotubes (MWNTs) based Pt electrodes (Pt/MWNTs) for oxygen reduction reaction (ORR) in polymer electrolyte membrane fuel cells (PEMFCs) are prepared by depositing Pt nanoparticles on electrochemically functionalized MWNTs with in situ ion exchange method. The morphology of the Pt/MWNTs electrode is characterized by a scanning electron microscope (SEM) and a transmission electron microscope (TEM). The chemical composition of the electrode is analyzed by X-ray photoelectron spectroscopy (XPS). The electrochemical activity is investigated with cyclic voltammetry (CV). Pt nanoparticles are highly dispersed on MWNTs. The electrochemical surface area of the ion-exchanged electrode (prepared with ion exchange) and the conventional electrode are 688.3 and 542.6 $cm^2\ mg^{-1}$ Pt, respectively. The Pt utilization, which is the ratio of the electrochemical surface area and the chemical surface area, is greatly enhanced on the ion-exchanged electrode (98.2%), as compared with 48.4% for the conventional one. The activity of the ion-exchanged electrode to ORR is higher than the conventional one. The increased Pt utilization and the improved electrocatalytic activity are attributed to the specific structure of the ion-exchanged electrode.

Keywords: PEM fuel cell; Carbon nanotube; In situ ion exchange; Electrochemical surface area; Pt utilization

1. Introduction

The polymer electrolyte membrane fuel cell (PEMFC) has attracted much attention due to its high-energy efficiency and no emissions. But its wide application is hindered by its high cost. It is generally believed that the large amount of platinum required as a catalyst in PEMFCs is one of the main reasons why fuel cells are excluded from commercialization. In the past two decades, many efforts have been devoted to increase the utilization of Pt and reduce the amount of Pt used in PEMFCs. These conventional efforts can be categorized into the following [1]: (1) to decrease the size of the Pt nanoparticles that loaded on carbon support [2]; (2) to improve the dispersion of Pt nanoparticles in the electrodes [3]; (3) to introduce the polymer electrolyte (e.g. Nafion ionomer) in the catalyst layer to enhance the proton transport [4]; (4) to introduce proton conducting sulfonic acid groups to the surface of the catalyst supports [5].

Conventional PEMFC electrodes are generally prepared with the so-called "hot-pressing" method [6]. The catalyst Pt/C is first prepared by impregnation-reduction or other methods; the mixed ink of the catalyst Pt/C and the Nafion solution is applied onto a backing support (e.g. carbon paper) by spraying, and then the resultant gas diffusion electrode is hot-pressed with a Nafion membrane. This precatalyzation procedure is also called "ex situ catalyzation" [7]. The common problems that encountered in the conventional electrodes are [8]: (1) protons can not access to the Pt nanoparticles that are isolated from polymer electrolyte Nafion; (2) the addition of Nafion in the catalyst layer tends to wrap some Pt nanoparticles and the carbon support, which leads to poor electron transport. It is said that up to 90% of the platinum catalyst in PEMFCs may be inactive [9]. In contrast, the in situ catalyzation of PEMFC electrodes can avoid or alleviate the above mentioned problems. The usually used method for in situ catalyzation is the electrochemical deposition (ECD). This process deposits Pt or Pt alloy catalysts only where both protons and electrons can access, thus theoretically it can improve the utilization of Pt. However, Pt nanoparticle sizes from ECD usually fall in the range of 20–70 nm [10]. The enhanced Pt utilization is barely realized.

* Corresponding author. Tel.: +86 451 86417853; fax: +86 451 86413707.
E-mail addresses: yuyan.shao@gmail.com (Y. Shao), yingphit@hit.edu.cn (G. Yin).

0378-7753/$ – see front matter © 2006 Elsevier B.V. All rights reserved.
doi:10.1016/j.jpowsour.2006.03.064

In this work, we developed a novel in situ ion exchange method for constructing PEMFC electrodes and greatly improved Pt utilization. An ion exchange method has already been used to prepare the carbon supported Pt catalyst [3,11]. In this technique, a platinum cation complex is ion-exchanged with H^+ ions of the acid functional groups on the surface of the carbon support materials, and then the ion-exchanged Pt cation complex is reduced to Pt nanoparticles in H_2 atmosphere. The ion exchange method usually gives a high Pt dispersion [3]. But when the ion-exchanged Pt/C is applied in the conventional electrode, it encounters the same problems mentioned above. The in situ ion exchange is expected to give a high Pt dispersion while avoiding the common problems.

Carbon nanotubes (CNTs) are employed as the catalyst support in this work. CNTs have attracted much interest for application as the catalyst support since their discovery, owing to their good mechanical and unique electrical properties and structure [12,13]. Multi-walled carbon nanotubes (MWNTs) are selected as the support rather than single-walled carbon nanotubes (SWNTs) because MWNTs are lower in production cost and higher in electrical conductivity than SWNTs [14]. CNTs supported Pt (Pt alloy) nanoparticles have shown enhanced catalytic activity to methanol electrooxidation [15] and oxygen reduction reactions (ORRs) [16]. The reasons for the higher performance of Pt/CNTs, as compared with carbon black supported Pt nanoparticles (Pt/C), can be listed as follows [17]: (1) the unique structure and electric properties of CNTs; (2) CNTs have few impurities, while carbon black (e.g., Vulcan carbon XC-72) contains significant quantities of organosulfur impurities, which can poison Pt metal [1]; (3) another problem in Pt/C is that some Pt nanoparticles are trapped in deep cracks of carbon black, which cannot work as catalysts of electrodes because the effective formation of the triple-phase boundary (gas–electrode–electrolyte) is essential for PEMFCs, CNTs do not have such cracks so that most Pt nanoparticles on CNTs are expected to be used as effective catalysts [18].

2. Experimental

2.1. MWNT-based electrode preparation

MWNT-based electrode was prepared as follows. First, MWNTs (purity $\geq$ 95%, 10–20 nm in diameters, 5–15 μm in lengths, from Shenzhen Nanotech Port Co. Ltd., China) were ultrasonically mixed with PTFE emulsion in Milli-Q ultrapure water (18.2 MΩ cm, Millipore); second, the mixed ink of MWNTs and PTFE was sprayed onto a teflonized carbon paper (PTFE 20 wt.%); then the resulted MWNT-electrode was sintered under 340 °C in air for 30 min. The spraying layer was of 3 mg cm^{-2} (mass fraction: MWNTs 95%, PTFE 5%).

2.2. Electrochemical functionalization of MWNT-electrode and Pt loading

Before Pt loading, the MWNT-electrode was electrochemically functionalized to generate the carboxyl on the surface of MWNTs. The electrochemical functionalization of MWNTs was performed in 0.5 mol L^{-1} H_2SO_4 in a three-electrode cell setup (see Section 2.4) [19] by 535 potential cycles between 0.05 and 1.4 V (vs. RHE) (≈8 h) with the scan rate of 0.05 V s^{-1}. The end-potential is 0.05 V. The up-potential of 1.4 V was selected because it was believed that carboxyl would be oxidized at potentials more positive than 1.4 V [20,21] and the structure of MWNTs would be irreversiblely destroyed at higher potential [22,23]. The electrochemically functionalized MWNT-electrode was washed with ultrapure water (18.2 MΩ cm) to remove the residue H_2SO_4 solution. Then the MWNT-electrode was immersed in the Pt precursor [15.0 mmol L^{-1} $Pt(NH_3)_2(NO_2)_2$ solution, Tanaka Precious Metals Group, Japan] for 48 h, with MWNT side exposed to the solution. The MWNT-electrode was then immersed in Milli-Q ultrapure water, stirred for 48 h (the ultrapure water was refreshed every 8 h) to remove the non-ion-exchanged $Pt(NH_3)_2(NO_2)_2$. And then the ion-exchanged Pt ions were reduced to Pt nanoparticles in H_2 at 190 °C.

The Pt loading was determined by the "burning method" [24]. The MWNT electrode (before Pt loading) and the Pt/MWNTs electrode were burned in air at ca. 800 °C, and the difference between the residues of the two burned samples was assumed to be the amount of Pt loading, which was 0.29 mg cm^{-2} (the total amount of Pt divided by the geometric area of the electrode).

For comparison, a conventional electrode was prepared by spraying the mixed ink of in-house-made Pt/MWNTs (Pt 20 wt.%) catalyst [25] and Nafion solution onto a teflonized carbon paper (PTFE 20 wt.%), with the same Pt loading (0.29 mg cm^{-2}) and a Nafion loading of 20 wt.% [19].

2.3. Physical characterization

The morphologies of the Pt/MWNTs electrodes were investigated by a scanning electron microscope (SEM) (Hitachi S4700). The in-house-made Pt/MWNTs catalyst used in the conventional electrode and the Pt/MWNTs scraped from the ion-exchanged electrode were characterized by transmission electron microscope (TEM, JEOL JEM-1200EX).

X-ray photoelectron spectroscopy (XPS) analysis was performed with a Physical Electronics PHI model 5700 instrument. The Al X-ray source operated at 250 W. The sample to analyzer takeoff angle was 45°. Survey spectra were collected at a pass energy (PE) of 187.85 eV over the binding energy range 0–1300 eV. High binding energy resolution Multiplex data for the individual elements were collected at a PE of 29.55 eV. During all XPS experiments, the pressure inside the vacuum system was maintained at 1×10^{-9} Pa.

2.4. Electrochemical measurements

Cyclic voltammetry (CV) was used to study the electrochemical properties of the Pt/MWNTs electrode. The CV measurements were conducted in a three-electrode cell setup as described in [19]. A reversible hydrogen electrode (RHE) and a Pt foil were used as the reference electrode and the counter electrode, respectively. Measurements were performed at a scan rate of 0.01 V s^{-1}. Before all CV experiments, the electrolyte solution

was saturated with Ar gas. The stable cyclic voltammograms were recorded after scanning for five cycles.

Oxygen reduction reaction (ORR) was performed in the same electrochemical cell. The working electrode was held vertically in a chamber filled with 0.5 mol L^{-1} H_2SO_4. O_2 (30 mL min^{-1}) was supplied to the carbon paper side and the catalyst side exposed to H_2SO_4 solution.

CV and ORR were both carried out at room temperature (20 ± 1 °C).

3. Results and discussion

3.1. XPS analysis

The electrochemically functionalized MWNT electrode is characterized with XPS. Fig. 1 shows the C1s spectra of the raw MWNT electrode and the electrochemically functionalized MWNT electrode. The spectra were each fitted into five individual component peaks, as shown in Table 1 [26–29]. It is clear that the oxygen-containing functional groups were formed on the surface of MWNT after electrochemical functionalization. The peak at 283.4 and 285.2 eV is attributed to the graphite carbon (C–C) and the hydrocarbons (C–H), respectively [28]. The spectral contribution of the carboxyl carbon peak increases from about 0 to 7.11% after electrochemical functionalization, which is necessary and advantageous for ion exchange [30].

Fig. 2 shows the Pt4f XPS spectra of the ion-exchanged electrode before (Fig. 2A) and after (Fig. 2B) reduction with H_2. The spectra show doublets containing a low energy band ($Pt4f_{7/2}$) and a high-energy band ($Pt4f_{5/2}$) which is centered at 3.33 eV higher than the low one. The area ratio of 4/3 for $Pt4f_{7/2}/Pt4f_{5/2}$ of each spectrum agrees well with literature values [31,32]. The peaks at

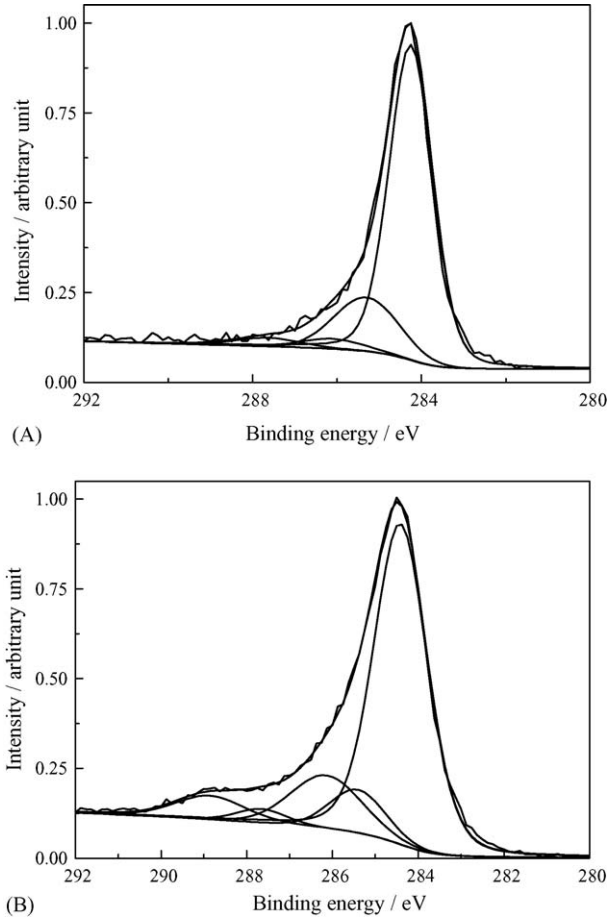

Fig. 1. C1s XPS spectra of carbon nanotube electrode before (A) and after (B) electrochemical functionalization (CV between 1.0 and 1.4 V for 8 h in 0.5 mol L^{-1} H_2SO_4, 20 ± 1 °C).

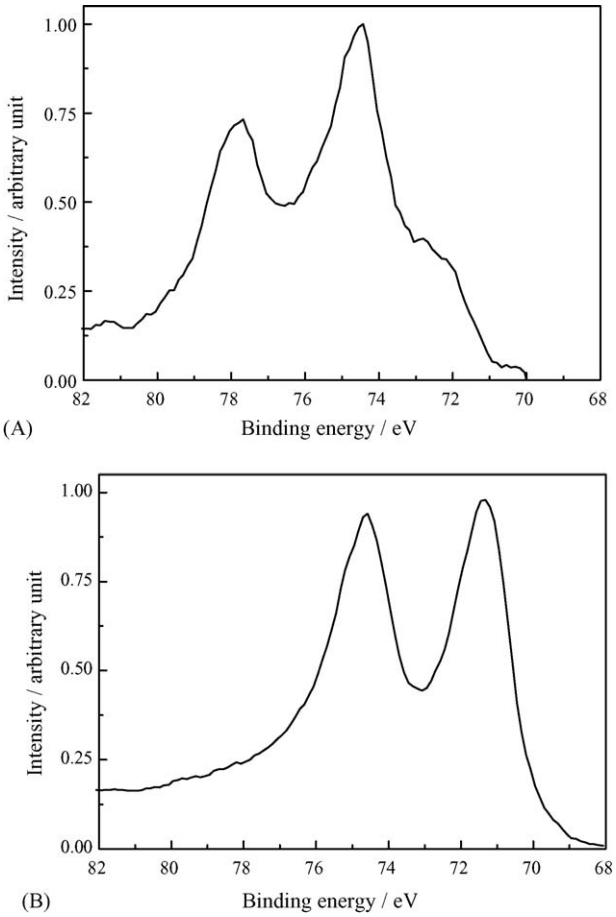

Fig. 2. XPS spectra of the ion-exchanged Pt/MWNTs electrode before (A) and after (B) reduction with H_2.

Table 1
Results of the fits of the C1s spectra, values given in % of total intensity

Sample[a]	COOH 288.4 eV[b]	C=O 287.6 eV	C–O 286.1 eV	C–H 285.2 eV	C–C 284.3 eV
AP-CNT	0.01	2.80	3.12	11.40	82.67
EF-CNT	7.11	2.67	12.95	8.68	68.59

[a] AP-CNT: as-prepared carbon nanotube electrode; EF-CNT: electrochemically functionalized carbon nanotube electrode.
[b] Binding energy [26,28,29,37].

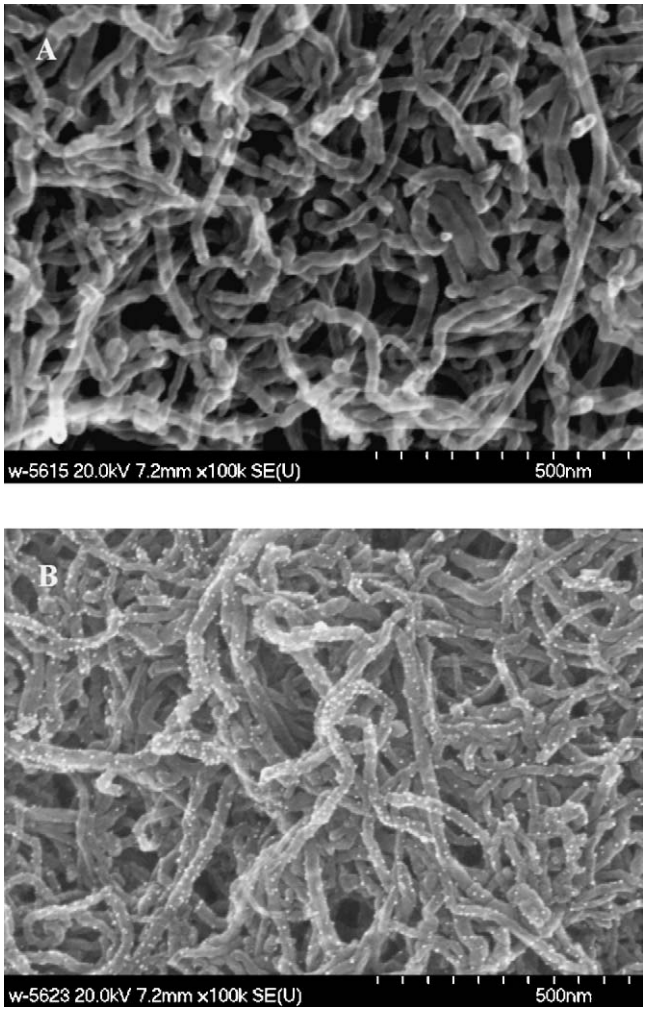

Fig. 3. SEM images of MWNT-electrodes before (A-left) and after (B-right) Pt loading with in situ ion exchange method. The highly dispersed bright nanoparticles on the image (B) are platinum as determined by EDXS (energy dispersive X-ray spectroscopy).

74.42 eV (Fig. 2A) and 71.29 eV (Fig. 2B) are assigned to Pt (II) in $[Pt(NH_3)_2]^{2+}$ [33] and Pt metal [31], respectively. This confirms that Pt was loaded on the electrode through ion exchange. The amount of platinum on the surface of the electrode can also be estimated from the XPS spectra (ca. 25 wt.%).

3.2. Electron microscopy characterization

Fig. 3 shows representative SEM images of the MWNT-electrodes before (A) and after (B) Pt loading by in situ ion exchange. It can be seen from the images that the diameters of MWNTs are around 20 nm. Pt nanoparticles are highly dispersed on carbon nanotubes.

Fig. 4 shows the TEM images of the ion-exchanged Pt/MWNTs and the conventional one. The distribution obtained with TEM image analysis is presented in the histogram in Fig. 5. The mean nanoparticle diameters for the ion-exchanged Pt/MWNTs and the conventional one are 4.0 and 2.5 nm, respectively. The mean nanoparticle diameter of the ion-exchanged Pt/MWNTs in this work is larger not only than the conventional one, but also than the previously reported Pt nanoparticles loaded on carbon black with ion exchange method [3]. This may be attributed to the incompleted removal of the non-ion-exchanged Pt cations.

3.3. Electrochemical activity

Fig. 6 shows the cyclic voltammograms of Pt/MWNTs electrode made by in situ ion exchange method (a) and conventional method (b). The electrochemically active surface area, also noted as electrochemical surface area (ESA, $cm^2\ mg^{-1}$ Pt) of the electrode can be calculated from the charge transfer (Q_H, $mC\ mg^{-1}$ Pt) for the hydrogen adsorption and desorption in the hydrogen region (0.05–0.4 V) of cyclic voltammograms [25,34]. The constant for ESA calculation is $0.21\ mC\ cm^{-2}$ and then the value of

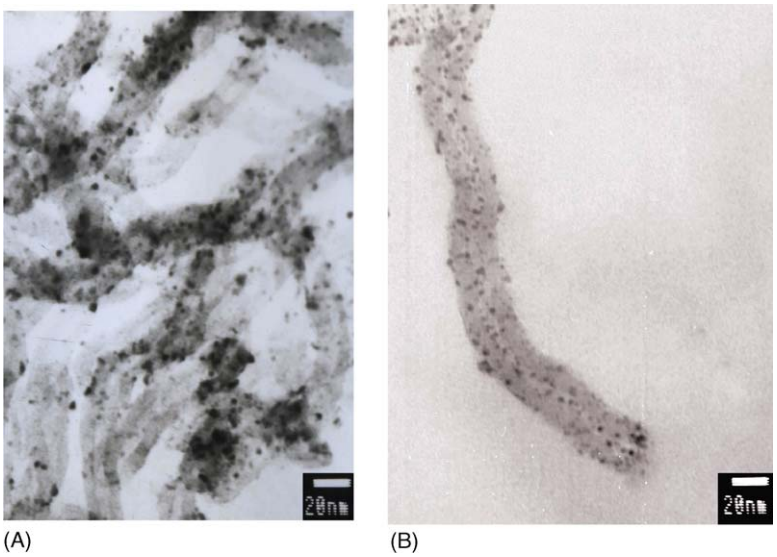

Fig. 4. TEM image of (A) ion-exchanged and (B) conventional Pt/MWNTs.

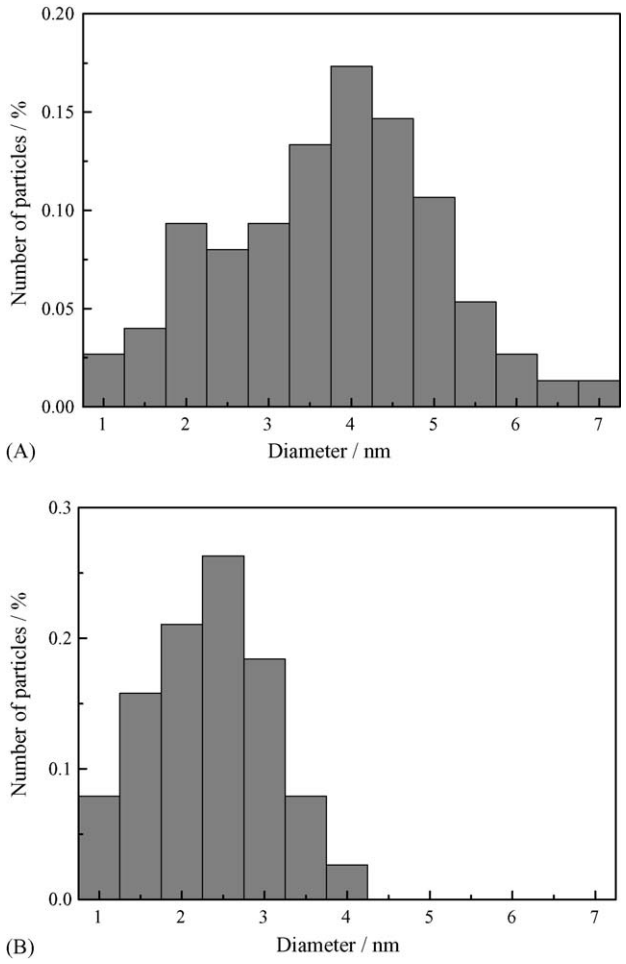

Fig. 5. Size distribution of Pt nanoparticles of Pt/MWNTs (A) ion-exchanged and (B) conventional one.

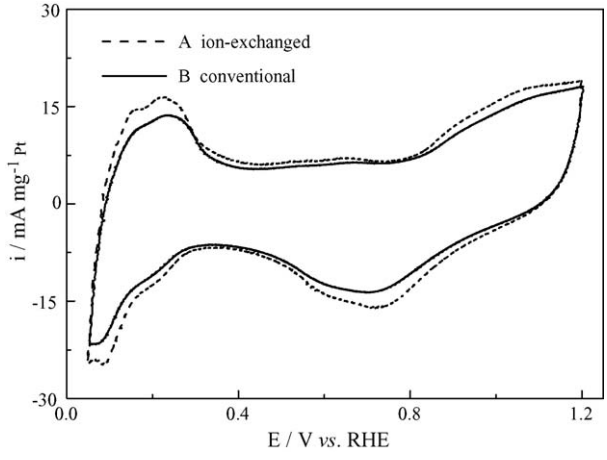

Fig. 6. Cyclic voltammograms of Pt/MWNTs electrode made by in situ ion exchange method (A) and conventional method (B). Electrolyte: 0.5 mol L^{-1} H_2SO_4; scan rate: 0.01 V s^{-1}; temperature: 20 ± 1 °C.

the ESA is obtained from:

$$\mathrm{ESA} = \frac{Q_\mathrm{H}}{0.21}$$

The ESA is one of the most important parameters for characterizing PEM fuel cell electrodes. A higher ESA implies a better electrode, as more catalyst sites are available for electrode reactions. The ESA for the ion-exchanged electrode and the conventional electrode calculated from the CVs shown in Fig. 6 are 688.3 and 542.6 $cm^2\ mg^{-1}$ Pt, respectively, with the former 1.27 times that of the later.

The chemical specific surface area (CSA, $cm^2\ mg^{-1}$ Pt) of Pt nanoparticles can be calculated from following equation with the assumption that all particles are in spherical shape [25,35]:

$$\mathrm{CSA} = \frac{60,000}{\rho d}$$

where ρ is the density of Pt (21.4 g cm^{-3}) and d (nm) is the mean diameter of the Pt nanoparticles in the catalyst. The CSA of the ion-exchanged electrode and conventional electrode are 700.9 and 1121.5 $cm^2\ mg^{-1}$ Pt, respectively. Here what we are interested in is the Pt utilization, which is defined as the ratio of the ESA and CSA, because it can tell how many surface Pt atoms are active in electrochemical reactions. It can be calculated that the Pt utilization on the ion-exchanged electrode and the conventional electrode are 98.2% and 48.4%, respectively, with the former more than two times the late.

The mean diameter of Pt nanoparticles (d), the electrochemical surface area (ESA), the chemical surface area (CSA) and the Pt utilization for both electrodes are summarized in Table 2.

The 98.2% Pt utilization on the ion-exchanged Pt/MWNTs electrode implies that almost all surface Pt atoms are electrochemically active. The conventional electrode encounters the common problems as described above. The Pt nanoparticles are partially isolated and separated from the external circuit, and these Pt nanoparticles are unavailable in electrochemical reactions. So, the Pt utilization for the conventional electrode is much lower.

The greatly enhanced Pt utilization on the ion-exchanged electrode can be explained as follows. It has been confirmed that Pt was loaded on MWNTs through ion exchange between $[Pt(NH_3)_2]^{2+}$ and H^+ on the surface of MWNTs which was produced during the electrochemical functionalization. The reaction can be tentatively formulated as the following:

$$[Pt(NH_3)_2]^{2+} + \mathrm{CNT\text{–}COOH} - [\mathrm{CNT\text{–}COO}]^- [Pt(NH_3)_2]^{2+}[NO_2]^- + H^+$$

where CNT–COOH is the carboxylic acid on MWNTs.

Table 2
The mean diameter of Pt nanoparticles (d), the electrochemical surface area (ESA), the chemical surface area (CSA) and the Pt utilization for the ion-exchanged and conventional Pt/MWNTs electrodes

Sample	d (nm)	ESA ($cm^2\ mg^{-1}$ Pt)	CSA ($cm^2\ mg^{-1}$ Pt)	Pt utilization (%)
Ion-exchanged	4.0	688.3	700.9	98.2
Conventional	2.5	542.6	1121.5	48.4

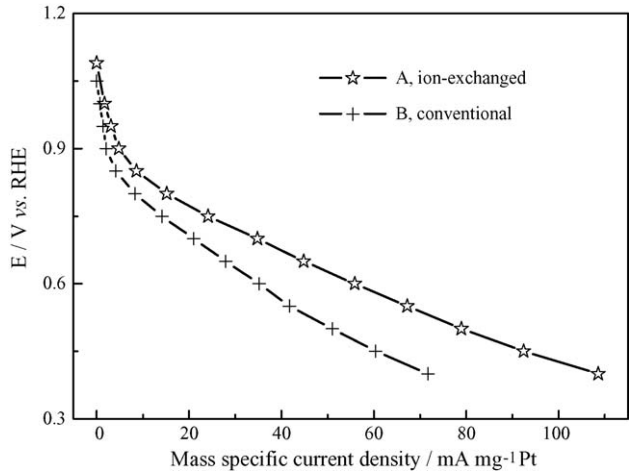

Fig. 7. Oxygen reduction on (A) ion-exchanged and (B) conventional Pt/MWNTs electrode. O_2 flow rate 30 mL min^{-1}, 20 ± 1 °C, ambient pressure.

The –COOH groups were electrochemically formed on the surface of MWNTs. Therefore, the sites of –COOH are proton- and electron-accessible. And so, the Pt nanoparticles loaded on these sites are electrochemically active, which results in a high Pt utilization (98.2%).

3.4. Oxygen reduction

Fig. 7 shows the ORR polarization curves on the Pt/MWNTs electrodes prepared with in situ ion exchange and conventional method. The ORR current densities for the ion-exchanged electrode at a given potential are larger than that on the conventional one, for example, at the potential 0.8 V, the mass specific current density on the ion-exchanged electrode is 15.2 mA mg^{-1} Pt, compared with 8.3 mA mg^{-1} Pt for the conventional electrode. This means that the ion-exchanged electrode has a higher catalytic activity to oxygen reduction. This is expected from the comparison of the electrochemical surface area of the two electrodes. However, the Pt particle size effect cannot be excluded. It was reported that Pt nanoparticles with a mean diameter of 3 nm showed the highest mass specific activity to ORR [36]. Considering that the Pt particle size of the ion-exchanged electrode is larger than 3.0 nm, we expect a still higher performance for the ion-exchanged electrode if the Pt particle size decreases. Further work is needed to optimize Pt particle size.

4. Conclusions

PEMFC electrodes usually suffer from Pt utilization loss due to the conventional electrode-preparation. Using an in situ ion exchange method, we have successfully constructed a PEMFC electrode with the MWNTs as the catalyst support. The electrode shows a larger electrochemical surface area and a higher Pt utilization than the conventional one. The electrocatalytic activity of the ion-exchanged Pt/MWNTs electrode towards oxygen reduction reaction (ORR) is higher than that of a conventional electrode. The improved Pt utilization and the electrocatalytic activity are attributed to the specific structure of the ion-exchanged Pt/MWNTs electrode, which guarantees that almost all Pt nanoparticles are deposited on the electrochemically active sites. This approach provides a new way to develop high-performance PEMFC electrodes.

Acknowledgment

This work was supported by Natural Science Foundation of China (No. 20476020).

References

[1] S. Litster, G. McLean, J. Power Sources 130 (2004) 61.
[2] X. Sun, R. Li, D. Villers, J.P. Dodelet, S. Desilets, Chem. Phys. Lett. 379 (2003) 99.
[3] K. Yasuda, Y. Nishimura, Mater. Chem. Phys. 82 (2003) 921.
[4] C.H. Hsu, C.C. Wan, J. Power Sources 115 (2003) 268.
[5] E.B. Easton, Z.G. Qi, A. Kaufman, P.G. Pickup, Electrochem. Solid-State Lett. 4 (2001) A59.
[6] E. Antolini, J. Appl. Electrochem. 34 (2004) 563.
[7] M.W. Verbrugge, J. Electrochem. Soc. 141 (1994) 46.
[8] X. Wang, M. Waje, Y.S. Yan, Electrochem. Solid-State Lett. 8 (2005) A42.
[9] S.D. Thompson, L.R. Jordan, M. Forsyth, Electrochim. Acta 46 (2001) 1657.
[10] H. Tang, J.H. Chen, Z.P. Huang, D.Z. Wang, Z.F. Ren, L.H. Nie, Y.F. Kuang, S.Z. Yao, Carbon 42 (2004) 191.
[11] E. Auer, A. Freund, J. Pietsch, T. Tacke, Appl. Catal. A-Gen. 173 (1998) 259.
[12] Z.L. Liu, X.H. Lin, J.Y. Lee, W. Zhang, M. Han, L.M. Gan, Langmuir 18 (2002) 4054.
[13] M.M. Waje, X. Wang, W. Li, Y. Yan, Nanotechnology 16 (2005) S395.
[14] C. Wang, M. Waje, X. Wang, J.M. Tang, R.C. Haddon, Y.S. Yan, Nano Lett. 4 (2004) 345.
[15] C. Kim, Y.J. Kim, Y.A. Kim, T. Yanagisawa, K.C. Park, M. Endo, M.S. Dresselhaus, J. Appl. Phys. 96 (2004) 5903.
[16] W.Z. Li, C.H. Liang, W.J. Zhou, J.S. Qiu, Z.H. Zhou, G.Q. Sun, Q. Xin, J. Phys. Chem. B 107 (2003) 6292.
[17] X.S. Zhao, W.Z. Li, L.H. Jiang, W.J. Zhou, Q. Xin, B.L. Yi, G.Q. Sun, Carbon 42 (2004) 3263.
[18] T. Matsumoto, T. Komatsu, H. Nakano, K. Arai, Y. Nagashima, E. Yoo, T. Yamazaki, M. Kijima, H. Shimizu, Y. Takasawa, J. Nakamura, Catal. Today 90 (2004) 277.
[19] Y.Y. Shao, G.P. Yin, Y.Z. Gao, Chin. J. Inorg. Chem. 21 (2005) 1060.
[20] Y. Yang, Z.G. Lin, J. Appl. Electrochem. 25 (1995) 259.
[21] S. Lefrant, M. Baibarac, I. Baltog, T. Velula, J.Y. Mevellec, O. Chauvet, Diam. Relat. Mater. 14 (2005) 873.
[22] G.U. Sumanasekera, J.L. Allen, S.L. Fang, A.L. Loper, A.M. Rao, P.C. Eklund, J. Phys. Chem. B 103 (1999) 4292.
[23] J.S. Ye, X. Liu, H.F. Cui, W.D. Zhang, F.S. Sheu, T.M. Lim, Electrochem. Commun. 7 (2005) 249.
[24] N.Y. Jia, R.B. Martin, Z.G. Qi, M.C. Lefebvre, P.G. Pickup, Electrochim. Acta 46 (2001) 2863.
[25] Y. Xing, J. Phys. Chem. B 108 (2004) 19255.
[26] K.J.H.U. Zielke, W.P. Hoffman, Carbon 34 (1996) 983.
[27] J. Diaz, G. Paolicelli, S. Ferrer, F. Comin, Phys. Rev. B 54 (1996) 8064.
[28] R.I.R. Blyth, H. Buqa, F.P. Netzer, M.G. Ramsey, J.O. Besenhard, P. Golob, M. Winter, Appl. Surf. Sci. 167 (2000) 99.
[29] H. Estrade-Szwarckopf, Carbon 42 (2004) 1713.
[30] Y.F. Jia, K.M. Thomas, Langmuir 16 (2000) 1114.
[31] J. Prabhuram, X. Wang, C.L. Hui, I.M. Hsing, J. Phys. Chem. B 107 (2003) 11057.
[32] Y.H. Lin, X.L. Cui, C. Yen, C.M. Wai, J. Phys. Chem. B 109 (2005) 14410.

[33] J.P. Contour, G. Mouvier, M. Hoogewys, C. Leclere, J. Catal. 48 (1977) 217.
[34] A. Pozio, M. De Francesco, A. Cemmi, F. Cardellini, L. Giorgi, J. Power Sources 105 (2002) 13.
[35] W.Z. Li, W.J. Zhou, H.Q. Li, Z.H. Zhou, B. Zhou, G.Q. Sun, Q. Xin, Electrochim. Acta 49 (2004) 1045.
[36] J.W. Guo, T.S. Zhao, J. Prabhuram, C.W. Wong, Electrochim. Acta 50 (2005) 1973.
[37] H.T. Fang, C.G. Liu, L. Chang, L. Feng, L. Min, H.M. Cheng, Chem. Mater. 16 (2004) 5744.